



## Research papers

# A methodological framework to assess PMP and PMF in snow-dominated watersheds under changing climate conditions – A case study of three watersheds in Québec (Canada)

Hassan Rouhani\*, Robert Leconte

Dept. of Civil Engineering, Université de Sherbrooke, 2500, Boulevard de l'Université, Sherbrooke J1K2R1, QC, Canada

## ARTICLE INFO

This manuscript was handled by Marco borgia, Editor-in-Chief, with the assistance of Daqing Yang, Associate Editor

## Keywords:

Probable maximum flood  
Climate change  
Canadian regional climate model  
Uncertainty analysis

## ABSTRACT

Climate change will affect precipitation and flood regimes. It is anticipated that the Probable Maximum Precipitation (PMP) and Probable Maximum Flood (PMF) will be modified in a changing climate. This paper aims to quantify and analyze climate change influences on PMP and PMF in three watersheds with different climatic conditions across the province of Québec, Canada. Output data from the Canadian Regional Climate Model (CRCM) was used to estimate PMP and Probable Maximum Snow Accumulation (PMSA) in future climate projections, which was then used to force the SWAT hydrological model to estimate PMF. PMP and PMF values were estimated for two time horizons each spanning 30 years: 1961–1990 (recent past) and 2041–2070 (future). PMP and PMF were separately analyzed for two seasons: summer-fall and spring. Results show that PMF in the watershed located in southern Québec would remain unchanged in the future horizon, but the trend for the watersheds located in the northeastern and northern areas of the province is an increase of up to 11%.

## 1. Introduction

There is agreement among scientists that the global temperature in the future will increase as a result of anthropogenic activities (DeWalle and Rango, 2008). According to the Intergovernmental Panel on Climate Change (IPCC), atmospheric temperature has already increased over the last decades in many parts of the world (Bates et al., 2008; Bernstein et al., 2007). As atmospheric temperature rises, the capacity of the atmosphere to hold water vapor increases according to the Clausius-Clapeyron equation (Jakob et al., 2008). Under such circumstances, it is likely that precipitation regimes will change. River runoff regimes are expected to change as well (Bates et al., 2008), although the direction of the change is difficult to predict as additional factors other than precipitation changes, such as the evaporation rate and soil moisture, can also influence flood magnitude. For instance, increasing precipitation and runoff have been predicted for future climate conditions in northern and central England (Arnell, 1998). By contrast, runoff in the Maude watershed in Western Europe is expected to decrease in future decades as a result of climate change (Menzel and Bürger, 2002). In the province of Québec, Canada, a study suggested that mean annual runoff is expected to increase by 9–15% at the 2050 horizon in the northern part of the province, while modest increases ranging from 1 to 5% are expected in the southern region (Desrochers

et al., 2008). This is in accordance with recent results of the Hydro-climatic Atlas of Québec, where future spring floods in higher latitudes of Québec are likely to increase, while in the south the trend would be reversed (CEHQ, 2015). In terms of mean annual temperature, it was found that the increasing trend in southern Québec is more significant than in central-eastern and western regions (Yagouti et al., 2008). This site-dependency of climate change was found for the annual maximum precipitation as well. For instance, daily annual maximum precipitation with a 20-year return period showed large increases in future climate conditions in southern Québec, but modest increases would occur in Atlantic Canada (Mailhot et al., 2012). Therefore, the evolution of hydrological regimes under climate change conditions should be studied at the regional scale.

Changes in river floods and design floods due to climate change have been investigated in numerous studies (Beauchamp et al., 2013; Milly et al., 2002; Stewart et al., 2005; Tofiq and Güven, 2015). In northern countries, where snow plays a dominant role in the hydrologic regimes of watersheds, the direction of changes in flooding regimes is less clearly defined, as increased temperatures will trigger midwinter thaws and affect the maximum snow water equivalent (SWE). Depending on the magnitude of the projected changes in precipitation, this could result in either increased or decreased risks of spring floods. For example, in a recent study in southern Québec (CEHQ, 2015), the

\* Corresponding author.

E-mail address: [Hassan.Rouhani@USherbrooke.ca](mailto:Hassan.Rouhani@USherbrooke.ca) (H. Rouhani).

daily spring peak flood with a 20-year period is expected to decrease in the southernmost part of the region (45° latitude) at the 2050 horizon, while an increase is projected in its northern part (50° latitude).

This paper focuses on estimating extreme flooding events under future climate conditions and, more specifically, the Probable Maximum Flood (PMF). This is a pressing issue as many hydraulic structures, such as dams, dikes and spillways, have been designed and are operated under the assumption of stationary hydrological conditions, which depend upon a stationary climate. Such conditions will no longer be valid (IPCC, 2012) as there is much evidence that, in many parts of the world, climatic and hydrological regimes are changing (AghaKouchak et al., 2012) and extreme hydrological events are occurring more frequently. For example, in the USA, the 1st percentile daily rainfall rate increased in the 1958–2011 time horizon (Groisman et al., 2013). In Canada, over the last 50 years, annual temperatures in Québec have increased by 1.2 °C (Vescovi et al., 2009). This province has also witnessed major floods over the last few decades, such as the Southern Quebec and Richelieu River spring floods and the Saguenay summer flood, which occurred respectively in 2017, 2011 and in 1996. The Southern Quebec flood affected 261 municipalities, forced the evacuation of 4000 people, flooded 5000 homes and damaged 400 roads. The Richelieu flood was a historical maximum (International Joint Commission, 2015) and it forced some 2000 people to leave their residences (Environment and Climate Change Canada, 2013). The Saguenay summer flood killed 10 people, forced 12,000 people to flee their homes and caused damage exceeding 800 million Canadian dollars. This flood was estimated as 8-times larger than a 100-year return period flood (Lapointe et al., 1998; Milbrandt and Yau, 2001). It was after this major flood that the government of Québec produced the Dam Safety Act and its attendant regulation, which came into effect in 2002. According to this Act, every large capacity dam must be able to withstand the PMF if the consequences of dam failure in flood conditions are classified as ‘severe’, i.e., when the affected area is occupied permanently by a population of 10,000 inhabitants or more (Gouvernement du Québec, 2015b). With the potential risk of PMF estimates changing under climate change conditions, it is necessary for dam owners to ensure that structures are safe for future climate conditions. Therefore, investigating the effects of climate change on PMF is critical in countries where laws are enforced based on this criterion for properly managing their hydraulic structures.

This paper is organized as follows. First, literature on PMF and climate change is presented and discussed. This is followed by a description of the methodology used to estimate the PMF for three watersheds in Québec, characterized by different climatic regimes and affected differently by climate change. The methodology is based on computing the Probable Maximum Precipitation (PMP). Traditionally, PMF is estimated by inserting PMP after a large storm when soil is nearly saturated (CEHQ and SNC-Lavalin, 2003; Prasad et al., 2011; Schreiner and Riedel, 1978), or by several random insertion of PMP in different days to take into account different soil moisture conditions (Beauchamp et al., 2013). In this study, PMP is estimated according to a novel approach by (Rouhani and Leconte, 2016). This approach is amenable to climate change impact studies. PMP is then used for summer-fall PMF estimation with taking into account different soil moisture conditions and spring PMF estimation with taking into account different snow and temperature conditions. Results and a discussion are then presented, followed by the conclusion.

## 2. PMF and climate change

PMF is the largest flood that can reasonably occur (Ely and Peters, 1984). This extreme flood is a result of critical meteorological conditions occurring simultaneously with favorable hydrological conditions (Beauchamp et al., 2013). Critical meteorological conditions are those that result in extreme precipitation. Favorable hydrological conditions are those that make the soil saturated. In regions with significant

annual snowfall, such as the province of Québec, there is also a risk of a severe flood when a significant amount of snow melts. Therefore, two types of flood scenarios can be defined in these regions: 1) summer-fall floods are the result of extreme rainfall on saturated soil, and 2) spring floods are the result of extreme rainfall on a very large amount of snow on the ground during an unusually warm period that produces the snowmelt. The extreme precipitation event that is usually used to estimate PMF is called the Probable Maximum Precipitation (PMP), which is defined as “the greatest depth of precipitation for a given duration meteorologically possible for a design watershed or a given storm area at a particular location at a particular time of year, with no allowance made for long-term climatic trends” (WMO, 2009). To study the impact of climate change on PMF, scenarios covering the summer-fall and spring seasons should be analyzed.

In recent years, an increasing number of researchers have investigated the influence of climate change conditions on extreme rainfall and floods (Condon et al., 2015; Groisman et al., 2005; Qian et al., 2010; Yagouti et al., 2008). One of the pioneering researchers was Robert A. Clark who studied key variables for PMP estimates, namely, maximum moisture, maximum inflow winds and precipitation efficiency (Clark, 1987). Clark also reported that the maximum moisture would increase as atmospheric temperature increases and would thus result in an increase in PMP values by at least 10% due to climate change (Clark, 1987). It was also predicted that extreme rainfall events over Europe would be more frequent under climate change conditions (Frei et al., 1998). Another study, using data from the Canadian Regional Climate Model (CRCM) (Caya and Laprise, 1999), established that extreme short duration rainfall events would be more intense in southern Québec (Mailhot et al., 2007). On the other hand, it was reported that short duration extreme rainfall events would be less intense in Alabama, USA (Mirhosseini et al., 2013). Potentially significant changes in runoff volumes and peak flows were also reported under future climate scenarios in southern Québec (Roy et al., 2001) and elsewhere (Arnell, 1998; Lagos-Zúñiga and Vargas M., 2014).

Since the study by Clark, few studies have been devoted to the impacts of climate change on PMP and PMF. A report by the World Meteorological Organization (WMO) briefly discusses potential changes in PMP under climate change conditions, emphasizing that atmospheric moisture availability, storm efficiency, depth-area curves and storm types should be analyzed in such investigations (WMO, 2009). It was reported that PMP is likely to increase under climate change conditions almost everywhere in the world (Kunkel et al., 2013). This study examined the effect of climate change on extreme rainfall events, maximum water vapor, horizontal wind and vertical air motion using projections of General Circulation Models (GCMs) towards 2071–2100. The researchers concluded that the probable causes of projected increases of PMP are changes in water vapor availability and the increase in extreme rainfall events due to the increasing trend of maximum precipitable water. These results were also asserted in an additional study (Lagos-Zúñiga and Vargas M., 2014) using GCMs, which reported that PMP is likely to increase in the Andean basins of Chile, leading to an increase in PMF of up to 175% by the years 2045–2065. An investigation on PMP values in southern Québec using Regional Climate Models (RCMs) confirmed that summer-fall PMP is likely to increase under climate change conditions in the 2041–2080 time horizon (Rousseau et al., 2014). Similar results for the 2071–2100 time horizon were obtained for a watershed located in central Québec, although no clear trend for future PMF was found (Beauchamp et al., 2013). Similarly, in the 2071–2100 time horizon, summer PMF values were reported not to show any clear trend for a watershed in Norway. However, fall PMF exhibited an increasing trend up to 15% (Chernet et al., 2013). Also, numerical weather models were used to investigate changes in PMP due to local to regional climate change caused by land use/land cover change. For example, the influence of reservoir size and irrigation on PMP of two watersheds in western USA was analyzed (Stratz and Hossain, 2014). In that study, the influence of water cycle

changes on regional climate through simulation of the dew point temperature using regional atmospheric modeling (RAMS) was studied. The dew point temperature was later used to estimate PMP. Results indicated that irrigation and reservoir size can notably affect PMP. In another recent study, numerical weather models were used to analyze climate change impacts on PMP using background temperature increases and also parameterizations such as cloud microphysics (Rastogi et al., 2017). A 20% increase of PMP estimate was found for south-western USA. Given the rather small number of studies dealing specifically with the effects of climate change on PMF, it is difficult to draw firm conclusions as to the direction of the projected changes. This is due to compounding factors, such as soil moisture and the maximum SWE, which are also affected by climate change and are decisive factors in establishing PMF values. The present paper proposes a methodology to estimate PMF under climate change conditions, based on estimating PMP according to an approach specifically adapted to climate change impact studies, and taking into consideration seasonal factors (i.e. soil moisture and snowpack conditions). The methodology is applied to three watersheds in Québec that are characterized by different physiographic and climatic features, which demonstrates its applicability to a variety of watersheds with snow-dominated hydrologic regimes.

### 3. Methodology

The basic approach to estimate the PMF under current and future climate conditions is to force a hydrological model with precipitation and air temperature projections derived from a regional climate model. The next sections detail the approach, beginning with a short description of the watersheds under study, the datasets and hydrological model used, and the methods to calculate PMP and PMF.

#### 3.1. Watersheds

Three watersheds were analyzed to investigate the influence of different climate conditions on PMP and PMF. As depicted in Fig. 1, the watersheds are in the province of Québec, Canada.

Although these three watersheds undergo long freezing seasons and mainly receive solid precipitation during winter, they have been selected to represent different climatic conditions in terms of precipitation and atmospheric temperature regimes, as shown in Table 1.

Overall, temperature and total precipitation decrease with increasing latitude. All three watersheds have hydrologic regimes dominated by snowmelt runoff, although summer storms can sometimes produce floods of a magnitude comparable to spring peak flows. The physiographic characteristics of the Chaudière, Moisie and Great Whale watersheds are presented in Table 1. The Chaudière watershed is located in southern Québec and has 180,000 inhabitants (Comité de Bassin de la Rivière Chaudière, 2015). Approximately 60% of the watershed is covered by forest, 30% is covered by agricultural land and the remaining area is devoted to industrial and residential activities. The Chaudière River, which flows north and into the St. Lawrence River, experiences the largest discharges in April, and sometimes comparable discharges occur in September. The mean annual flow in the outlet of the Chaudière watershed is 114 m<sup>3</sup>/s.

The Moisie watershed is located in the center of Québec. Its main watercourse is the Moisie River, which flows south and discharges into the Gulf of St. Lawrence. Around 4000 people live in this watershed (Gouvernement du Québec, 2015a). The area has very limited industrial/agricultural development and is mainly covered by forest. The Moisie River usually experiences the largest discharges in May. The mean annual flow in the outlet of the Moisie watershed is 410 m<sup>3</sup>/s.

The Great Whale watershed is located in northern Québec. Its main watercourse is the Great Whale River. The Great Whale watershed is mainly covered by forest. The Great Whale River, which flows westward and empties into Hudson Bay, usually experiences the largest discharges in June, and sometimes another comparable peak occurs in

the fall. The mean annual flow in the outlet of the Great Whale watershed is 514 m<sup>3</sup>/s.

Fig. 2 shows the average daily runoff hydrographs for the 1960–2005 period for these watersheds. The watersheds exhibit different hydrological regimes as a result of different physiographic and climatic characteristics. The Chaudière watershed has the smallest peak value and is also the smallest of the three watersheds. The peak flow in the Chaudière watershed usually occurs in April, while the peak flow usually occurs in May and June for the Moisie and Great Whale watersheds, respectively. The Moisie watershed has the largest peak value among the three watersheds, although its surface area is half that of the Great Whale. This is because of the annual snow received by the Moisie, which exceeds that of the Great Whale, with respective values of 400 mm and 240 mm. Also, the average temperature in the Moisie watershed during the melting season is 6.5 °C, which exceeds the value of 3.5 °C in the Great Whale watershed. The spring melt is therefore more intense on average over the Moisie watershed as compared to the Great Whale.

#### 3.2. Data

Observed flow and meteorological data required for calibrating the hydrological model (described below) come from the Centre d'expertise hydrique du Québec (CEHQ, now Direction de l'expertise hydrique) and from the National Land and Water Information Service (NLWIS) database, respectively. The NLWIS database provides grids of daily precipitation and the maximum and minimum surface temperature of Canada south of 60° latitude, with a resolution of 10 km, covering the years 1961–2003. These grids were interpolated daily from Environment Canada station observations using a thin plate smoothing spline surface fitting method (Hutchinson et al., 2009). Using interpolated values was necessary as very few weather stations with long and continuous precipitation and temperature data are currently available for the Moisie and Great Whale watersheds. Although there are several meteorological stations in the Chaudière watershed and its vicinity, NLWIS interpolated data were also used to maintain coherency. A daily precipitation comparison between NLWIS and a ground station (St. Prosper) in Chaudière watershed between 1970 and 2000 indicated mean values are only 2% different. Physiographic data sets (topography, soil type, vegetation cover, etc.) required by the model were obtained from two datasets, namely Geogratis (Natural Resources Canada, 2015) and Webarchive (International Institute for Applied Systems Analysis, 2015). Geogratis was used for land-use data (residential, industrial, forest, agriculture etc); and Webarchive was used for different soil types (i.e. different soil characteristics) in the watersheds of interest.

This study aims to estimate PMP and PMF under current and future climate conditions. As such, climate projections are required. To that end, climate models can simulate an array of 'equivalent' meteorological stations, along with vertical profiles of atmospheric variables, and can generate long 'historical' and future data series. In addition, output climate variables from these models are internally coherent since they are generated in the same system of solving mass and energy equations. It follows that the current and future climate projections are also coherent, enabling a study of the evolution of PMP and PMF as climate conditions shift by directly comparing simulated current and future values. Although Global Climate Models (GCMs) can simulate large rainfall events (Durman et al., 2001), Regional Climate Models (RCMs) are better suited to simulate such events at the watershed scale and, therefore, are preferred for hydrological studies. For example, general consistency between observations and the Canadian Regional Climate Model (CRCM) (Paquin, 2010) confirmed the ability of the CRCM to generate extreme storm events. CRCM output has been compared with observational data in a number of studies. For instance, Intensity-Duration-Frequency (IDF) curves in southern Québec were retrieved from CRCM output and compared favorably with IDF curves

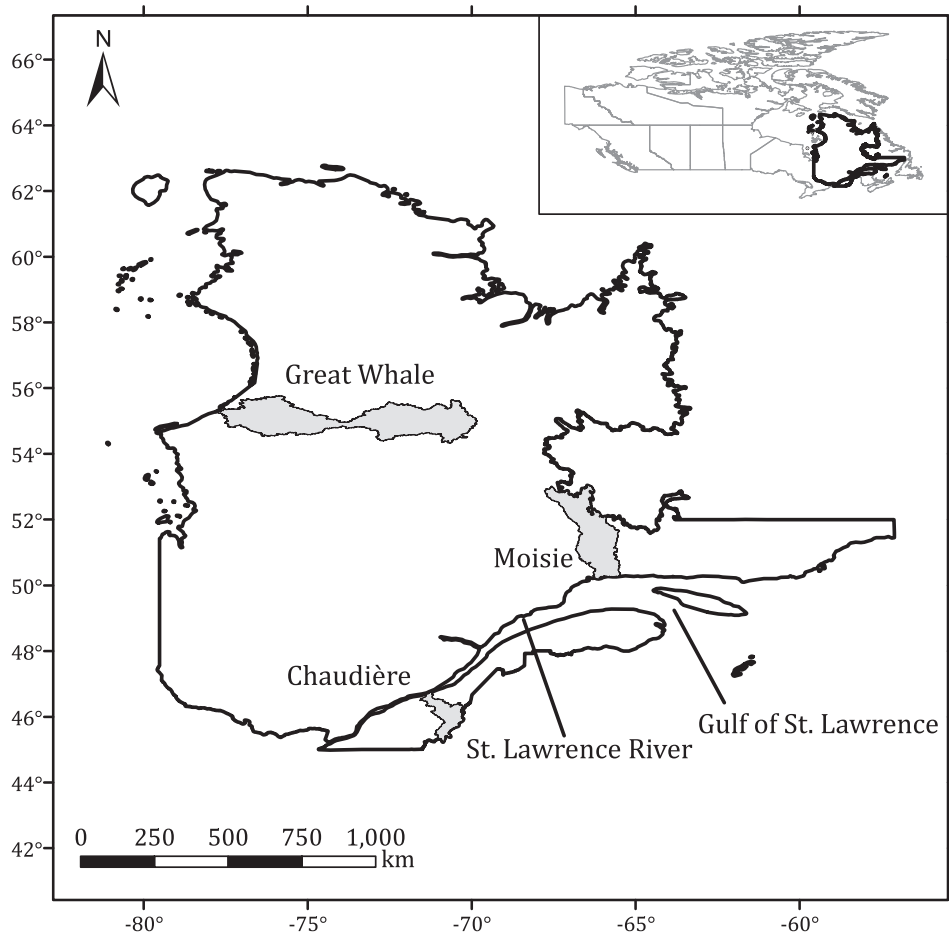


Fig. 1. Geographical location of three watersheds of interest in the province of Québec, Canada (adapted from Rouhani and Leconte, 2016).

**Table 1**  
Physiographic and hydroclimatic conditions of three watersheds under study (Environment Canada, 2015).

Watershed characteristics	Chaudière Lat: 45° to 47° N Long: 70° to 72° W		Moisie Lat: 50° to 53° N Long: 65° to 67° W		Great Whale Lat: 54° to 56° N Long: 70° to 78° W	
Area (km <sup>2</sup> )	6682		19,197		42,700	
Elevation (m)	Max.: 1300	Mean: 400	Max.: 1090	Mean: 550	Max.: 800	Mean: 340
24 h 100-year precip. (mm)	95		110		85	
100-year flood (m <sup>3</sup> /s)	2000		3500		2150	
Annual rain (mm)	892		728		409	
Annual snow (mm)	300		400		240	
Annual mean daily temp. (°C)	4.2		1		−4	

derived from observations (Mailhot et al., 2007). Its capacity to reproduce extreme observed events outside of Canada was also positively tested (Goyette et al., 2001). Moreover, it was reported that CRCM simulations of precipitable water are promising in terms of similarity with observations, although some underestimates were noticed in warmer seasons (Rousseau et al., 2014). It was therefore decided to use CRCM outputs as the prime data set to carry out this work due to the richness and completeness of such a database. Since the capacity of reproducing rainfall events is model dependent (Langousis et al., 2016), it was decided to include several climate simulations, thus allowing

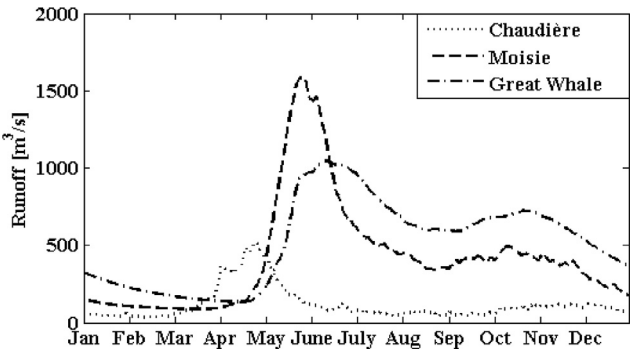


Fig. 2. Average hydrograph at the outlet of the watersheds.

uncertainty analyses (Mailhot et al., 2012). To this end, data used in this study were retrieved from CRCM version 4.2.3 (Paquin, 2010), driven by the following GCMs: (i) CGCM 3.1v2 (4th member) (de Elía and Côté, 2010; Music and Caya, 2007), (ii) CNRM-CM3 (Salas-Méila et al., 2005) and (iii) ECHAM 5 (Roeckner et al., 2003). The greenhouse gas (GHG) emission scenarios used to run GCMs are either SRES-A2 or A1B (Nakicenovic et al., 2000). Details of these different climate simulations can be found in Table 2. A total of seven climate simulations were used in this study. This selection of climate models enables investigating the influence of GCM structure (three models) and climate variability (five different initial conditions of a GCM, here the CGCM3). The effect of different GHG emission scenarios can also be studied as there are two emission scenarios.

Specific humidity in different atmospheric pressure levels (either 18

**Table 2**  
CRCM v 4.2.3 climate simulations used in this study.

Simulation	Current	aeY	aeZ	afa	afx	aeV	agw	agx
	Future	afb	afc	afd	afx	aeV	ahb	agx
GHG emission scenario		A2	A2	A2	A2	A2	A1B	A2
Atmospheric nesting data		CGCM 3	CGCM 3	CGCM 3	CGCM 3	CGCM 3	CNRM-CM3	ECHAM 5
Member number		1	2	3	4	5	–	–

or 23 depending on the model), surface atmospheric temperature, Convective Available Potential Energy (CAPE), SWE, daily maximum and minimum temperature and total precipitation in daily time steps were obtained at a spatial resolution of 45 km by 45 km for two 30-year long time horizons: 1961–1990 (recent past or reference) and 2041–2070 (future).

Climate models are known to be biased (i.e. the models systematically underestimate or overestimate some climatic variables) (Hempel et al., 2013; Schmidli et al., 2006). Therefore, bias removing is a common practice in studies involving climate models. Bias removal techniques try to lessen the difference between statistical moments (such as the monthly average) of observational data and climate model outputs and are supposed to preserve climatic trends. In this study, no bias removal modification was applied as it was deemed to damage the internal coherency of outputs. This is because bias removing requires observational data which is scarce for variables such as SWE, precipitable water and CAPE. Therefore, applying bias removal techniques to some selected variables (such as precipitation and temperature) and using the others “as is” (such as precipitable water and CAPE) harms the credibility of CRCM as an ensemble of climate data. One may argue that correcting biases for temperature and precipitation would result in a better timing and magnitude of the simulated flood. This is not an issue here as the concern is more on simulating *changes* in PMF magnitude consecutive to climate change, rather than providing absolute magnitude and timing. This is later discussed in the paper. On the other hand, CRCM outputs of precipitable water were “confirmed” by a comparison against observational data that were available for the Moisie watershed to lend reliability for using CRCM output in this study. Details of this comparison can be found in Rouhani and Leconte (2016).

### 3.3. Hydrological modeling

The SWAT hydrological model (Neitsch et al., 2002) was used to compute PMF. SWAT is a semi-distributed hydrological model. Processes simulated by SWAT include, infiltration, evapotranspiration, runoff, groundwater and snow accumulation and melt (Haguma, 2013). Sub-watersheds and the hydrographic network are automatically delineated by using a digital elevation model (DEM). SWAT further subdivides the watershed into Hydrological Response Units (HRU). HRUs are land portions with unique topographic, land-use and cover and soil characteristics (Arnold et al., 2012). Hydrological processes are calculated at the HRU level followed by an aggregation at the sub-watershed level. The resulting runoff is routed through the computed hydrographic network until reaching the main watershed outlet. Inputs to SWAT also include pesticide, nutrient, fertilizer database and septic system data. These analyses were not done in the present study. The calculations are carried out at a daily time step interval.

CRCM tiles were assumed as virtual meteorological stations for modeling current and future PMF. A calibration on daily time step based on observational data of precipitation and runoff in a period of 11 years was used for the Chaudière, Moisie and Great Whale watersheds. The corresponding validation period was 4, 10 and 10 years. The Nash-Sutcliffe (NS) criterion (Nash and Sutcliffe, 1970) applied to daily runoff values was used as the objective function to calibrate SWAT with the shuffled complex evolution algorithm (Duan et al., 1992). Calibration and validation results are presented in Table 3. Another

**Table 3**

Nash-Sutcliffe values for three watersheds in calibration and validation period.

Watershed	Calibration	Validation
Great Whale	0.82	0.72
Moisie	0.68	0.61
Chaudière	0.70	0.64

calibration scheme was also tried in this study by comparing observed versus simulated runoff from SWAT when directly forced by CRCM precipitation and temperature. This scenario did not produce promising results as dynamics of CRCM data are different than those of observational data and CRCM runoff still suffers from inconsistencies.

Overall, SWAT was able to adequately simulate the hydrological regime of the three watersheds. The calibrated model was driven with current and future climate projections generated by the CRCM model and PMP calculated from CRCM data to generate corresponding PMF values.

### 3.4. PMP

In this study, a deterministic approach to calculate 24-h PMP was applied based on simulated climate data from the CRCM. The method is based on the moisture maximization approach recommended by the WMO (WMO, 1973; WMO, 1986; WMO, 2009):

$$PMP = P_{obs} * \frac{W_{max}}{W_{storm}} = P_{obs} * r \quad (1)$$

In Eq. (1),  $r$  is the maximization ratio,  $P_{obs}$  is the maximum observed precipitation depth,  $W_{max}$  is the maximum precipitable water at the same time of year and same location as  $P_{obs}$  and  $W_{storm}$  is the actual precipitable water of the observed storm  $P_{obs}$  (WMO, 1973; WMO, 1986; WMO, 2009). To obtain precipitable water, the most accurate approach is to take humidity measurements at different atmospheric levels and sum them up, for example by using data collected by radiosondes (Schreiner and Riedel, 1978). In this study, precipitable water was instead calculated using simulated specific humidity from the CRCM database:

$$W = \frac{1}{g} \int_{P_1}^{P_2} q(P) dP \quad (2)$$

where  $W$  is the atmospheric moisture (precipitable water),  $g$  is the gravitational acceleration,  $q$  is specific humidity and  $P$  represents pressure.  $W_{storm}$  was calculated as the maximum precipitable water that occurred in a two-day period prior to and during the storm (Beauchamp et al., 2013; Rousseau et al., 2014).  $W_{max}$  can be estimated by different methods. If the observation record is long enough (at least 50 years), the maximum in the record can be used as  $W_{max}$ . However, this is rarely the case. In this study,  $W_{100}$ , the 100-year return period precipitable water, was taken as a representative value for  $W_{max}$  according to Beauchamp et al. (2013) and Rousseau et al. (2014). The statistical distribution used to calculate  $W_{100}$  is the General Extreme Value (GEV) distribution. This distribution has been recommended for annual maximum rainfall (Koutsoyiannis, 1999) and precipitable water distributions (Chow and Jones, 1994a). Thus, the maximization ratio

corresponds to:

$$r = \frac{W_{100}}{W_{\text{storm}}} \quad (3)$$

To estimate  $W_{100}$ , a time series of the annual maximum of precipitable water values was established. In the ‘traditional’ method, each element of this time series is the maximum recorded precipitable water at the same location as  $P_{\text{obs}}$  for the same period of each year (WMO, 2009). It is suggested to limit the maximization ratio by an upper bound to avoid overestimation. Different values for the upper limit have been suggested but there is a lack of a sound physical basis. Therefore, the validity of these values under climate change conditions can be questioned. Instead of imposing an upper limit on the maximization ratio, a different approach was adopted to build the time series of maximum precipitable water from which  $W_{100}$  is retrieved. Briefly, each element of this time series is the maximum among precipitable water values in each year for which selected climate variables resemble those of  $P_{\text{obs}}$ . Climate variables of  $P_{\text{obs}}$  are estimated based on the data before and during the storm. Climate variables used in this study include atmospheric temperature at the surface and CAPE, which are considered indicative of conditions leading to significant storm events. Details of the approach can be found in (Rouhani and Leconte, 2016). As this approach is not constrained by setting an upper limit on the maximization ratio, and because it attempts to preserve the original storm dynamics in calculating  $W_{100}$ , we postulate that it is better suited to calculate PMP under climate change conditions as opposed to the traditional method (Rouhani, 2016).

The PMP approach was applied to estimate the summer-fall and spring PMP for current and future climates at each CRCM tile of the region encompassing each of the three watersheds under study. The area covering each watershed was established in a manner to maximize the number of CRCM “virtual meteorological stations” that are subject to a direct PMP transfer to the watershed under study.

The largest value for the PMP obtained in each watershed and surrounding area (in case of transferability) was considered as the representative PMP value for the corresponding watershed. The seasons’ initial and final dates were established based on the geographical location of watersheds (see Table 1) that also indicates different precipitation patterns, where summer-fall extreme rainfalls are typically larger than spring events (CEHQ and SNC-Lavalin, 2003). The summer-fall season starts on May 16th in the Chaudière and June 16th in the Moisie and Great Whale watersheds and ends on November 30th. It is also possible to define seasons based upon snow on the ground (Foulon et al., 2017; Klein et al., 2016; Rousseau et al., 2014). However, in this study calendar dates were used to enable comparison between two same-length seasons.

### 3.5. PMF

PMF is obtained by combining critical meteorological and hydrological conditions. One approach for estimating summer-fall PMF is to force a hydrological model with a large precipitation event to produce saturated soil conditions, followed by a PMP (CEHQ and SNC-Lavalin, 2004; Rousseau et al., 2012). Recently, statistical approaches have been developed to better reflect the influence of different soil moisture levels on PMF (Beauchamp et al., 2013; Paquet et al., 2013). In such methods, a distribution of PMF values is obtained as opposed to a unique value. These methods do not require establishing initial conditions prior to the PMP. In this study, a method inspired by Beauchamp et al. (2013) was used to calculate a distribution of summer-fall PMF for the current and future climates. Basically, the PMP computed for each watershed was inserted in each day of a precipitation/temperature time series and the resulting runoff was simulated and counted as a ‘potential’ watershed PMF. The precipitation and temperature time series were obtained from the CRCM simulations under current and future climate conditions. Although quantification of soil moisture was not possible in this study,

this approach allowed covering the entire range of possible soil moisture conditions that actually happened in the watersheds during the time horizons under study.

The resulting PMF values were ranked and a representative value, in this case the 90th percentile value, was selected as the watershed PMF. There are different thresholds for identifying extreme values, such as the 99th percentile for temperature (e.g. Mishra et al. 2015). In this study, the 90th percentile was inspired by a definition of extreme climate conditions: an event which is higher/lower than the tenth percentile (Karl et al., 1996). However, using other values based on PMF percentiles is possible according to the judgment of engineers, managers or decision makers. The temporal evolution of PMF distributions according to future climate scenarios will indicate how climate change influences PMF values.

For spring PMF, an alternative methodology was used. Spring PMF results from the melting of a deep snowpack during an unusually warm period along with extreme rainfall. Therefore, three hydro-meteorological variables/events come into play for establishing the PMF. Here, a single ‘critical’ combination of the three factors has been adopted, leading to the production of a single PMF value, rather than a distribution. The occurrence of three maximized events (snowpack, temperature and rainfall) simultaneously is unrealistic and may cause overestimates (Debs et al., 1999; Hydro-Québec and SNC-Shawinigan, 1992). Instead, two possible scenarios were defined: (i) a PMP was estimated and was combined with a 100-year SWE ( $S_{100}$ ), and (ii) 100-year rainfall ( $P_{100}$ ) was combined with the Probable Maximum Snowpack Accumulation (PMSA). It is worth mentioning that non-stationarity of time-series can be explicitly taken into account for estimating 100-year return period events (e.g. Rousseau et al. (2014) and Klein et al. (2016) for more details). In the current study in 30-year time horizons were assumed to be stationary. However, the probability density functions obtained for the different time horizons selected in our study did not have the same parameter values, hence reflecting non-stationarity between the horizons. Using CRCM, PMSA has recently been shown to be subject to variations as climate changes (Klein et al., 2016). This justifies the application of a second scenario in this study. For the first scenario, annual maximum SWE values were retrieved from CRCM output, from which  $S_{100}$  was estimated. The air temperature time series should be established in a way that reflects an extreme, yet realistic, warm period. The method selected followed that of Debs et al. (1999). It typically begins with a warm temperature period which ripens the snowpack, followed by a second warm period which produces the snowmelt. Eventually, the scenario ends with a colder temperature series that includes a rainfall event (Debs et al., 1999). A two-week melting period is recommended to be sufficient in the province of Québec; however, it can be shortened or extended when it is necessary to do so (Debs et al., 1999). The temperature values during the melting period were estimated through statistical analyses of observed air temperature to obtain a 100-year air temperature time series ( $T_{100}$ ) according to (Chow and Jones, 1994a). For the second scenario, PMSA was calculated for current and future climate conditions and inserted along with  $P_{100}$  to calculate corresponding PMF. One approach to calculate PMSA is to sum up maximized and non-maximized storms that would occur in a winter season that experienced large snow accumulations. Storm maximization is based on moisture maximization similar to estimating PMP. Only storms with maximum precipitation efficiency are maximized. This estimation procedure should be repeated on several severe winters, and the largest snow depth after maximization among these winters is the PMSA (Klein et al., 2016; CEHQ and SNC-Lavalin, 2004; Chow and Jones, 1994b; Debs et al., 1999). However, a modified version of this approach was adopted for the following reasons. First, precipitation efficiency is a difficult and complex quantity for definition and estimation (Gao and Li, 2008) and therefore poses a challenge to properly identify maximizable storms. To circumvent this difficulty, Debs et al. (1999) selected as storms to be maximized those events which produced more than 5 cm of snow accumulation. This

criterion does not guarantee that selected storms are efficient. The second reason is that we believe this approach is prone to overestimate PMSA as it is highly unlikely that several maximized storms occur in the same season, especially if storms to maximize are selected based on low snow accumulations. Instead, the following approach was used to construct the PMSA. First, the five largest winters in terms of snow accumulation are selected in each time horizon. For each winter selected, the three largest storms are identified and maximized, from which the largest maximized storm is kept, regardless of the time of occurrence in the season. This maximized storm is then added to the snowpack before the thaw begins. The winter with the largest maximized snowpack produces the PMSA.

As mentioned above, SWAT is a semi-distributed hydrological model. Therefore, unlike lumped models, precipitation needs to be spatially distributed at the watershed scale. In this study, the elliptical pattern approach for rainfall events proposed by the WMO (WMO, 2009) was used to spatially distribute PMPs which are calculated at the CRCM tile scale. In the elliptical method, the direction of the ellipses was found by trial and error to obtain the direction that yields the most severe flood. The eye of the storm, which is also the center of the ellipses, was positioned at the centroid of the watershed, yielding the largest areal precipitation mean, and thus, the most severe flood. Finally, the PMP value set at the centroid of each watershed to compute PMF was the maximum value among the PMPs estimated over all CRCM tiles covering the watershed and its surroundings. In other words, it was assumed that the computed PMP could be directly transposed to the watershed centroid. More details can be found in Rouhani (2016).

#### 4. Results

Results are presented for summer-fall and spring seasons. The largest PMF value obtained is defined as the all-year PMF.

##### 4.1. Climate change scenarios

Since PMP and watershed hydrology are closely linked to seasons, data analysis was performed on a seasonal basis. Projected daily precipitation and temperature plots are presented in Fig. 3 for the three watersheds and two future time slices (reference and future). In this figure, for each time horizon, median values of seven climate simulations described in Table 2 are displayed.

Fig. 3 shows that for each watershed, the CRCM projections produce a temperature increase. This increase can be up to 7 °C, depending on the season and watershed considered. The temperature increase is larger in colder months than in warmer ones. For precipitation, a 5% decrease was obtained in the summer-fall season for the future time horizon in the Chaudière, while for the Moisie and Great Whale watersheds, an increase up to 14% was obtained. Modest increases are noted in the winter in the Moisie and Great Whale watersheds, while a larger augmentation is observed in the Chaudière watershed. In general, the increase in temperature and precipitation is more pronounced at high latitudes. This is in accordance with various studies (Bernstein et al., 2007; Karl et al., 2008; Solomon et al., 2007).

##### 4.2. summer-fall floods

In Fig. 4, summer-fall PMP values in three watersheds for two time horizons are displayed. The box plots correspond to PMP variability due to climate-related uncertainties as represented by the different climate scenarios. As can be seen in this figure, PMP tends to increase in the future for all three watersheds. Also, PMP values decrease at higher latitudes. This is because the atmosphere holds less water vapor in higher latitudes according to the Clausius-Clapeyron equation. Therefore, less severe storms occur in higher latitudes, as confirmed by 100-year rainfall values for the Chaudière, Moisie and Great Whale watersheds, see Table 1. In addition, PMP values from different climate

models tend to converge for both current and future climates at higher latitudes, as denoted by a narrower range of the corresponding box plots.

The summer-fall PMF was estimated first by inserting a PMP in all simulation days of the corresponding time horizon. This produced a distribution of large flood events from which a PMF value was extracted. In this study, the value corresponding to the 90th percentile of the cumulative distribution was considered as representative of summer PMF. Cumulative distribution functions (cdf) of extreme flood events (including PMF) for the three watersheds and two time horizons can be found in Fig. 5. Each cdf displays variability resulting from different soil moisture conditions which naturally evolve and vary along the summer-fall season. Considering seven climate simulations, an array of cdf curves of extreme flood events for each watershed and time horizon is obtained, reflecting uncertainty due to GCM structure, climate variability and the GHG emission scenario. As can be seen in this figure, for all three watersheds, the range of possible PMFs widens and shifts rightward in the future. In other words, summer-fall PMF is most likely to increase in the future. Moreover, moving toward higher latitudes renders a narrow range of possible PMF values and this can be interpreted as decreasing climate-related uncertainties (model, natural variability and GHG emission scenarios) in higher latitudes, in accordance with decreasing PMP variability, see Fig. 4. Increasing PMF uncertainty from the current to future climate is observed for all three watersheds, which is in accordance with Fig. 3, where T and P uncertainty increases in the future.

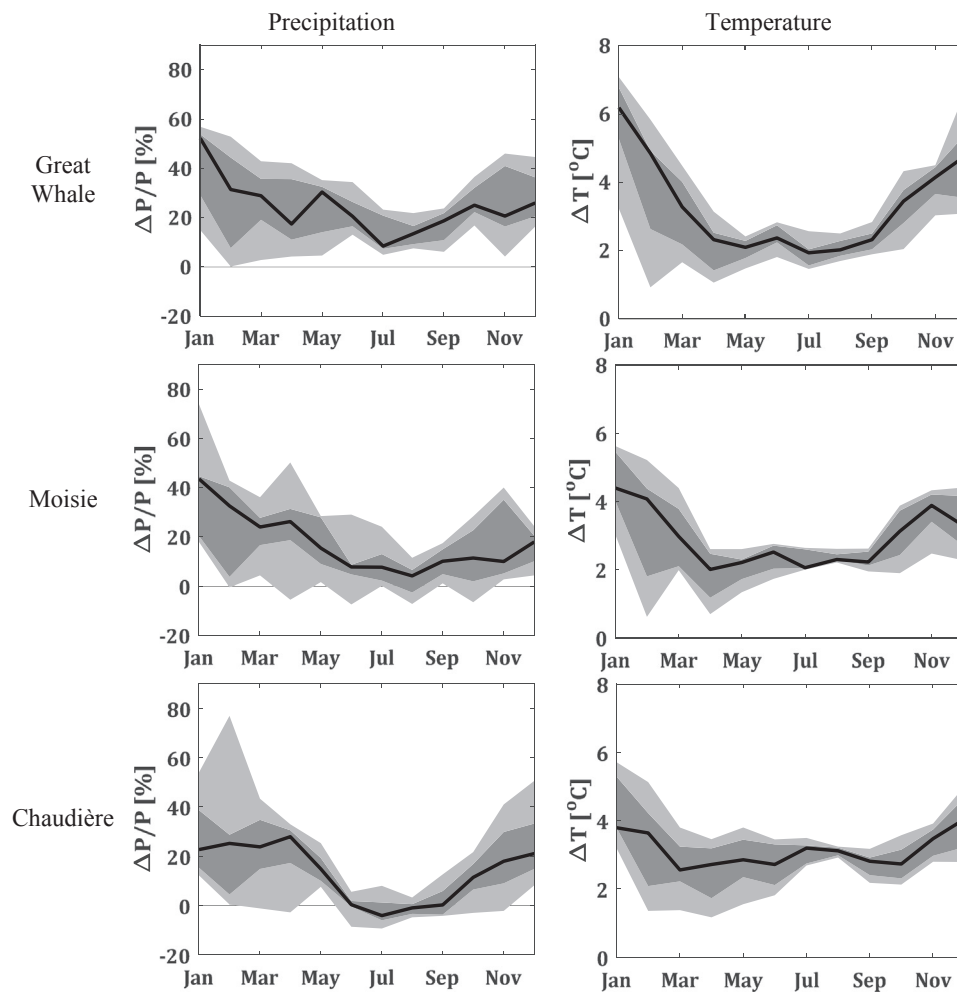
Fig. 5 allows distinguishing the influence of climate-related uncertainty due to climate model structure, natural climate variability and the GHG emission scenario through selected PMP values, from uncertainty due to soil moisture conditions on the resulting PMF. More specifically, the range of PMF values for a given cdf curve displays PMF variability due to soil moisture, whereas the lateral spread of all cdf curves corresponds to variability due to the climate-related uncertainties. Note that the cdf curves for a given watershed and time horizon all tend to be parallel, meaning that the effect of soil moisture on PMF tends to be similar, no matter what climate scenario is used. The figure also reveals that uncertainty due to soil moisture tends to outweigh uncertainty due to climate scenarios as the watershed is located at higher latitude.

##### 4.3. Spring floods

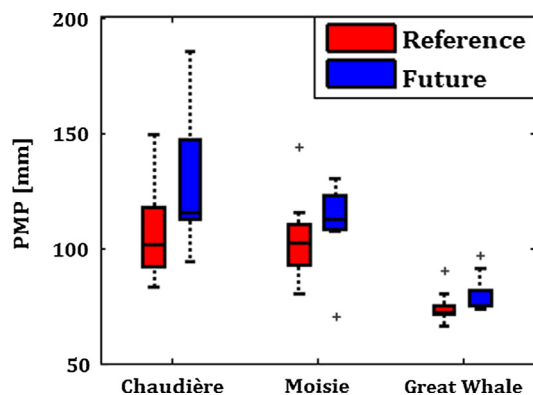
The spring PMF was obtained according to two scenarios. The first scenario was forcing a hydrological model with the largest PMP estimate in the watershed for each climate model, along with  $S_{100}$  as an initial condition in the model and a 100-year time series of air temperature,  $T_{100}$ , to melt the snowpack (SC1). The second scenario was forcing a hydrological model with a 100-year return period rainfall,  $P_{100}$ , along with Probable Maximum Snow Accumulation (PMSA) and  $T_{100}$  (SC2). The length of the temperature series was adjusted (extended or shortened) to capture the largest possible flood.

Fig. 6 represents the driving forces for computing spring PMF, i.e. extreme snow water equivalent ( $S_{100}$  and PMSA), extreme rainfall (PMP and  $P_{100}$ ) and critical air temperature time series ( $T_{100}$ ) represented here as an average value over the melting time period, for the two scenarios described above and for the current and future climate. The variability displayed in the box plots is the result of climate related uncertainties (model structure, natural climate variability and GHG emission scenario).

Fig. 3 shows that the temperature rises in future climate conditions, as well as the precipitation in winter months. In lower latitudes, this temperature rise will convert solid precipitation events to rainfall. Consequently, solid precipitation is reduced by 10% in the Chaudière watershed (median value), while it is slightly increased by 1 and 0.5% in Moisie and Great Whale, respectively. This, in turn, reduces  $S_{100}$  and PMSA, see Fig. 6. Temperature is expected to rise in the future, so will



**Fig. 3.** Projections of precipitation and temperature in three watersheds. The precipitation projection is displayed as the difference between the future precipitation and reference period, normalized by reference period. The temperature projection is displayed as the difference between the future temperature and reference period. The light gray shade refers to 5–95 percentile, dark gray shade refers to 25–75 percentile and medians are displayed as solid black lines.



**Fig. 4.** Summer-fall PMP values for three watersheds and two time horizons. Center, upper and lower lines are 50, 75 and 25th percentiles, respectively. Whiskers are 95 and 5th percentiles and outliers are displayed separately by a '+'.

$T_{100}$ , see Fig. 6. These changes in rainfall, SWE and  $T_{100}$  will in turn affect future spring PMF in a way that depends on the relative contributions of the individual driving forces, as seen in Fig. 7, which shows the range of possible spring PMF values reflecting, for each individual watershed, climate-related uncertainties. As can be seen in the figure, spring PMF values remain stable for the Chaudière watershed

while they tend to increase under future climate conditions in higher latitudes for both investigated scenarios. This is mainly the result of increasing SWE (both  $S_{100}$  and PMSA) in the northernmost watersheds (see Fig. 6). Meanwhile, SWE tends to decrease in the future in the Chaudière watershed, as the comparatively smaller increase in winter precipitation (see Fig. 3) is counterbalanced by increasing midwinter thaw events resulting from a warmer winter. Moreover, Fig. 7 shows that, for all studied watersheds, the second scenario (PMSA +  $P_{100}$ ) produced larger PMF values as compared to the first scenario (PMP +  $S_{100}$ ) for both current and future climates. This is because the difference between PMSA and  $S_{100}$  is much larger than the one between PMP and  $P_{100}$ .

Therefore, the second scenario was kept for the determination of the spring PMF. This is contrary to findings by Debs et al. (1999), where scenario 1 (PMP +  $S_{100}$ ) produced the largest PMF in their study of the Ste-Marguerite watershed, located close to the Moisie watershed. However, Debs et al. (1999) used a 3-day PMP that includes a 204-mm rain in a 24-h period, which is more than twice the 24-h PMP used in our study (95% value of 97 mm, see Fig. 6), which explains why their PMP +  $S_{100}$  scenario produced the largest PMF value. The Ste-Marguerite and Moisie results are discussed further in section 5.

## 5. Discussion

Results of this work indicate that the PMF in Québec's watersheds will undergo changes as the climate shifts. The overall change for both

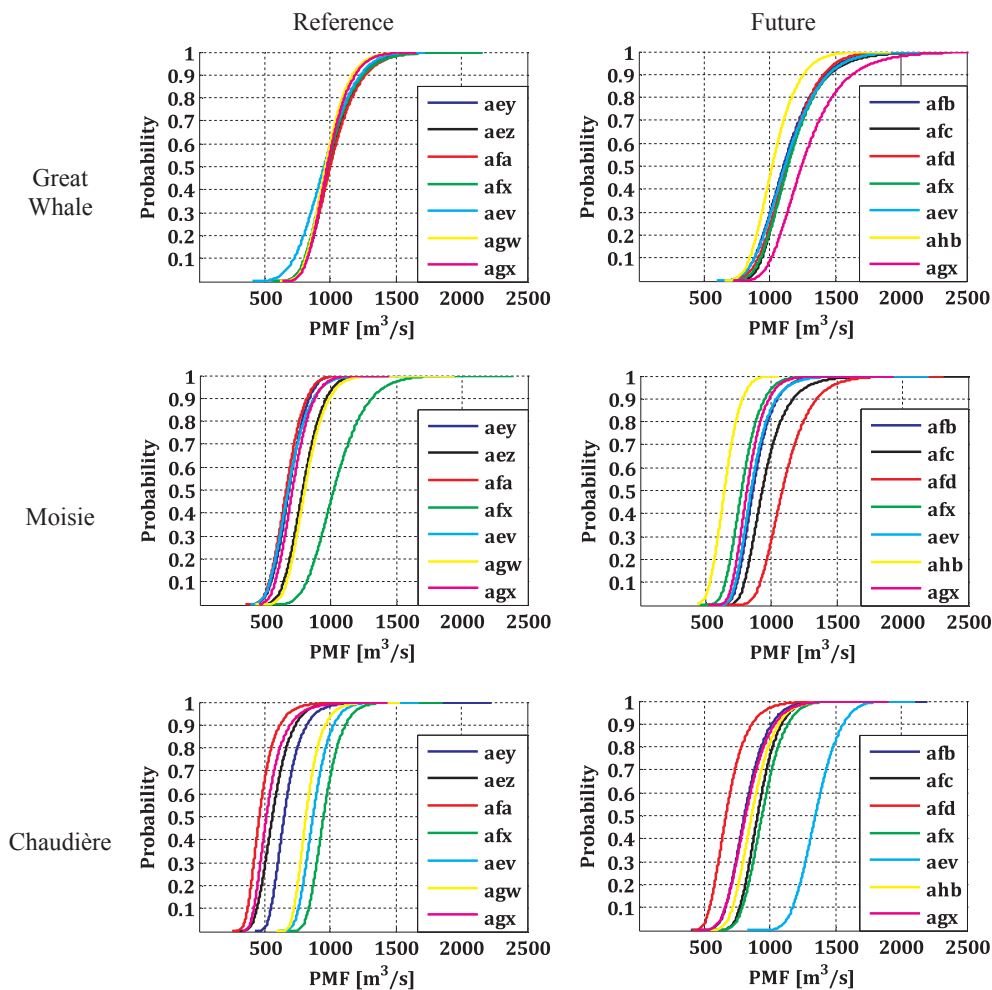


Fig. 5. Cumulative distribution functions of PMF values in three watersheds.

spring and summer-fall PMF is computed according to the following equation:

$$\Delta \text{PMF} = 100 * (\text{PMF}_{\text{future}} - \text{PMF}_{\text{reference}}) / \text{PMF}_{\text{reference}} \quad (4)$$

which helps to reduce the effect of inherent model (climate and hydrological) biases (Minville et al., 2008).

As seen in Figs. 5 and 7, the spring PMF will surpass the summer-fall PMF for all watersheds considered and all time horizons (reference and future). In other words, simulation results indicate that the PMF in a future climate will still be governed by a combination of rainfall and snowmelt processes. Furthermore, the impact of climate change on PMF will differ with latitude. Average spring PMF of the Chaudière watershed, located in the southern part of the province, will only be marginally affected by a changing climate (3% increase), as increasing rainfall will be outweighed by a decreasing snowpack resulting from the warmer air temperature. Watersheds located in the northernmost areas would have an average future spring PMF increase of 8 and 11%, respectively for the Moisie and Great Whale watersheds, as both the rainfall and snowpack will be increasing.

A different procedure was used to calculate the summer-fall PMF in order to account for the impact of soil moisture on the magnitude of the design flood. According to this procedure, a distribution of PMF values was obtained for each climate scenario (see Fig. 5). The 90th percentile value of the cumulative distribution, reflecting a high soil moisture content, was considered as representative of summer-fall PMF and was used in Eq. (4) to calculate the shift in PMF due to climate change separately for each climate scenario (see Fig. 8). As can be seen in this figure, all summer-fall PMF values follow an increasing trend, except

for two models in the Moisie watershed. The average summer-fall increase in PMF is 31, 13, and 17%, for the Chaudière, Moisie and Great Whale watersheds, respectively. Contrary to the spring PMF, no trend exists with the watershed latitude. This is perhaps not surprising, given the significant influence of soil moisture on PMF and the complex interactions between soil moisture and temperature/precipitation regimes.

These results were obtained through a climatic-hydrological modeling process and, therefore, are subject to climate-related uncertainties (model structure, natural climate variability, GHG emission scenarios) as well as the hydrological model's structure and calibration. Two interrelated questions thus arise: 1) what confidence can be placed in the values of the PMF obtained? and 2) what confidence can be placed in the temporal trends obtained due to climate change?

Providing an answer to these two questions is a challenging task because the PMF is a conceptual flood, in other words, the theoretically largest flood resulting from a combination of the most severe meteorological and hydrologic conditions that could conceivably occur in a given area. It is therefore virtually impossible to validate a PMF. Its value will be disproven only once it is surpassed by a real flood. An additional challenge is that future climate scenarios are uncertain. Climate models represent the state-of-the-art in simulating future climatic regimes. However, there is no method of validating the climate simulations produced by these models. The 'goodness' of climate models at simulating current and future climate regimes is the subject of controversy, as some researchers consider all climate models as equally good (Scholze et al., 2006), while others believe that verification of natural systems is impossible (Oreskes et al., 1994; Petersen,

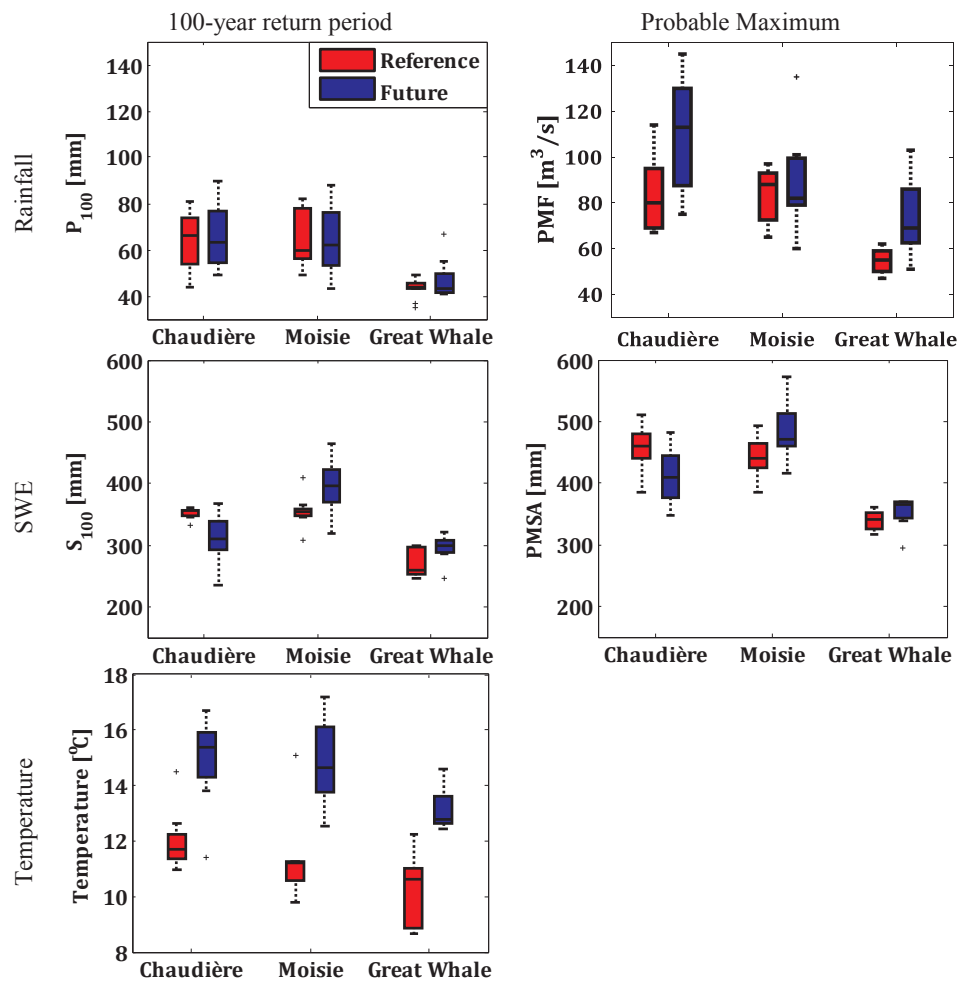


Fig. 6. Evolution of driving forces of spring PMF in three watersheds. In all panels, red and blue colors refer to reference and future time horizons, respectively. (For interpretation of the references to colour in this figure legend, the reader is referred to the web version of this article.)

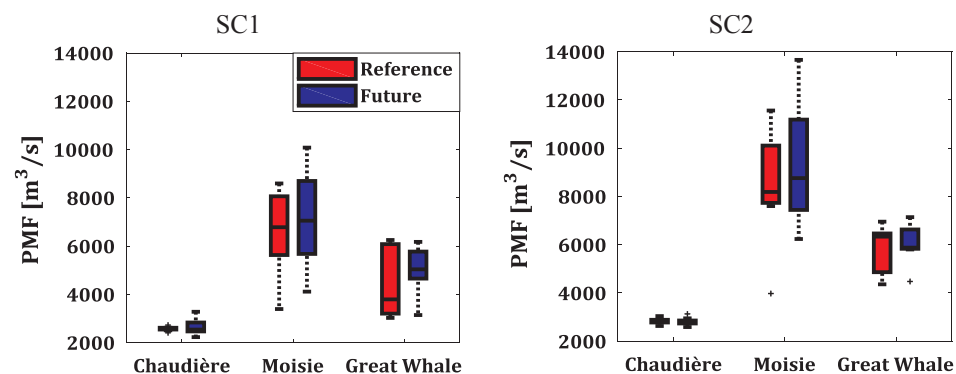


Fig. 7. Spring PMF values for three watersheds and two time horizons.

2000). Some researchers claim every model is definitely false (Morgan et al., 1992; Stainforth et al., 2007). Consequently, the best way to help answering the above questions is to carry out a full uncertainty analysis of the modeling process. In a study by Chen et al. (2011), the largest source of uncertainty in the hydrological impacts of climate change was attributed to the structure of climate models (Chen et al., 2011). In our study, seven climate scenarios were used in an attempt to better understand uncertainties due to climate model structure, natural climate variability and GHG emissions, on PMF. Therefore, a range of potential scenarios can be the best ‘representative’ of future PMF values. Other sources of uncertainties that are known to affect the estimation of

future hydrological regimes, and therefore PMF estimates, such as hydrological model structure and calibration (only one hydrological model was used) and downscaling approach (only one regional model was used) were not addressed in our study. Consequently, the climate scenarios used in this study provide an incomplete portrait of the sources of uncertainty affecting spring and summer-fall PMF. This is perhaps best reflected in Fig. 7, where the box-plots display an asymmetry in the distribution of spring PMF values, particularly for the Great Whale watershed. More climate scenarios are thus required to better quantify uncertainty so that the average PMF obtained from such an analysis would be more representative of the ‘true’ PMF.

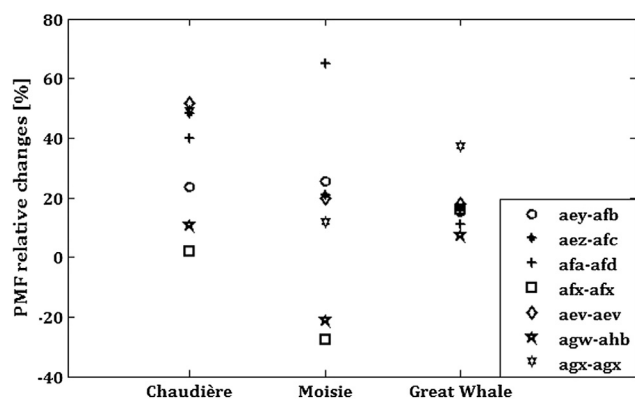


Fig. 8. Relative changes of summer-fall PMF in three watersheds.

Furthermore, the negative summer-fall PMF trends obtained with two climate models for the Moisie watershed, which affect the computed average trend, are linked to outliers in both current and future PMP estimates (see Fig. 4). This further points out the necessity of adding more climate scenarios for better defining future PMF.

A related issue is that climate models, including the CRCM, are typically biased. As mentioned above, bias was not removed to preserve the coherency of data and also because of observational data scarcity. Therefore, it is possible that PMP, PMSA,  $T_{100}$ ,  $P_{100}$  and  $S_{100}$  values derived from CRCM output are affected by biases and uncertainties resulting from the CRCM structure. Note that Chen et al. (2011) concluded that downscaling techniques (i.e. regional climate models, statistical downscaling) had a significant impact on the simulated average spring peak flow. This further reinforces the need to increase the number of climate scenarios to better address this source of uncertainty in evaluating spring PMF in watersheds dominated by snow processes. As noted above, analyzing climate change impacts as trends, rather than as absolute values, diminishes the effects of model biases on results.

Another way to provide some level of confidence as to the validity of the PMF values obtained in this study is to compare them with estimates from other studies carried out in the same regions. One such study is that of Debs et al. (1999) who calculated the PMF of the Sainte-Marguerite watershed, which is located just east of the Moisie watershed. These authors calculated the PMF of the watershed by combining a PMP with  $S_{100}$ , and also PMSA and  $P_{100}$ , as was done in this study. Table 4 compares the results of Debs et al. (1999) with our study for the two scenarios combining extreme precipitation and snowpack.

As shown in Table 4, the Moisie watershed is three times larger than the Sainte-Marguerite watershed. Depending on which scenario is taken, the Moisie/Sainte-Marguerite PMF ratio is either smaller (scenario 1) or larger (scenario 2) than the watershed area ratio. Considering scenario 1, the Moisie/Sainte-Marguerite PMF ratio is 1.70 (0.53 if divided by area), suggesting that the PMF in the Moisie

watershed may be underestimated relative to that of the Sainte-Marguerite watershed. Since  $S_{100}$  is similar in both watersheds (354 mm vs. 404 mm), the main reason for the mismatch between the PMF values is the PMP estimates, which are shown in Table 4. However, comparing the PMP from the two watersheds must be done with caution, as the PMP developed by Debs et al. (1999) is for a three-day storm, while a one-day PMP was developed in this study. With scenario 2, the Moisie/Sainte-Marguerite PMF ratio is 4.04 (1.28 if divided by area), this time suggesting overestimation of PMF in the Moisie. However, the PMF ratio was calculated with an average PMF value from the climate scenarios analyzed. Using the 25 percentile PMF value ( $7000 \text{ m}^3/\text{s}$ , see Fig. 7), a PMF ratio of 3.29 (1.06 when divided by area) was obtained, which is close to the watershed area ratio. It is therefore difficult to ascertain whether there is an overestimation of PMF in the Moisie watershed, and more climate scenarios are required to draw more definitive conclusions.

Also, although both studies used the WMO approach to estimate the PMP, the databases used for the studies significantly differ: this study used the CRCM output data, including a large storm, over an area encompassing the Moisie watershed, while the Debs et al. (1999) study analyzed 18 major storms which were maximized and transposed both spatially and temporally. Moreover, it is known that CRCM underestimates precipitation in cold months (Rouhani and Leconte, 2016). However, the fact that the  $S_{100}$  values in both studies are of comparable magnitude gives some confidence in using the CRCM output data as snowpack ‘observations’. To conclude, the comparative analysis between the Debs et al. (1999) study and our study did not provide any evidence that the PMF estimated for the Moisie watershed was either over or underestimated.

Note in Table 4 that the model averaged PMSA calculated for the Moisie watershed is notably less than that obtained by Debs et al. (1999). As well, the average PMSA of the Chaudière watershed is less than that obtained by Klein et al. (2016) for the Yamaska watershed, which is located not far from the Chaudière. Moreover, the range of PMSA values spanned 385–515 mm in the Chaudière, which is narrower compared to the 443–724 mm range obtained by Klein et al. (2016) for the Yamaska. These differences are attributed to different estimation approaches used in the current study and in Debs et al. (1999) and Klein et al. (2016), as described above.

A generalized method to estimate PMP based on the WMO approach for storm maximization and transposition has been developed for the province of Québec (CEHQ and SNC-Lavalin, 2003) using storms that have occurred over eastern Canada (i.e. Maritimes, Québec and Ontario provinces). The method, referred to as the SNC method, relies on the use of diagrams, tables and graphs to generate PMP estimates for a specific region. Table 5 compares spring and summer-fall PMP estimates (average values) from the SNC method and the approach used in this study. Table 5 indicates that using the CRCM data may be underestimating the PMP relative to estimates of the PMP using observations of major storms.

Again, since the ‘true’ value of the PMP cannot be assessed, a part of the observed difference may be attributed to an overestimation of the PMP using the SNC method and/or to an underestimation with the CRCM approach. Estimates of the PMF should therefore be interpreted with caution.

The PMP approach used here avoids the need to put an upper bound

Table 4

Comparison between results from this study and results for an adjacent watershed.

	This study average values	Debs et al. (1999)	Ratio
Watershed	Moisie	Sainte-Marguerite	3.09
area	19197 km <sup>2</sup>	6200 km <sup>2</sup>	
SC1 PMP	83 mm (one day)	250 mm (three days)	0.34
$S_{100}$	354 mm (CRCM)	404 mm (observation)	0.89
PMF	6600 m <sup>3</sup> /s	3986 m <sup>3</sup> /s	1.70
(PMF/area)	(29.7 mm/day)	(55.5 mm/day)	(0.53)
SC2 $P_{100}$	65 mm (one day)	77 mm (three days)	0.78
PMSA	442 mm (CRCM)	764 mm (observation)	0.59
PMF	8485 m <sup>3</sup> /s	2127 m <sup>3</sup> /s	4.04
(PMF/area)	(38.1 mm/day)	(29.6 mm/day)	(1.28)

Table 5

Comparison between results from this study and from SNC-Lavalin.

	Chaudière			Moisie			Great Whale		
	This study	SNC	Ratio	This study	SNC	Ratio	This study	SNC	Ratio
Spring	85	230	0.36	83	170	0.48	54	95	0.56
Summer-fall	107	270	0.39	104	185	0.56	75	120	0.62

on the maximization ratios recommended in the original WMO approach. Since the calculation of the maximization ratios is based on using atmospheric variables closely related to storm formation, the proposed approach is deemed more suitable for climate change studies. Figs. 4–7 present the temporal evolution of the PMP and PMF from the reference period to future (2041–2070) time horizon, respectively for the summer-fall and spring seasons. As a warmer atmosphere has an increased capacity to hold water vapor, one expects the PMP to increase with climate change. Figs. 4 and 6 confirm that the PMP increases over time for the three studied watersheds. As explained above, the computed PMF also changes from the control period to future time horizons and the direction of the changes is closely related to interactions between the PMP and soil moisture (for summer-fall PMF) and  $S_{100}$  and  $T_{100}$  events (for spring PMF) used in the hydrological modeling process. Moreover, trend analyses offer the advantage that uncertainties due to the model structure (climate and hydrology) are minimized. Therefore, we believe that the results presented in this study provide a plausible evolution of the PMF due to climate change. For instance, our study showed that the average increase in the spring PMF using PMP and  $S_{100}$  (SC1) was 8 and 11% between the 1961–1990 and the 2041–2070 time horizon, respectively for the Moisie and Great Whale watersheds. Clavet-Gaumont et al. (2017) also used SC1 and obtained an 11% increase for the Manic-5 watershed, geographically located between the Moisie and the Great Whale watersheds.

As mentioned above, a decreasing trend in the summer-fall PMP was obtained for two climate scenarios (afx-afx and agw-ahb, see Table 2) over the Moisie watershed. A decrease in PMP as the atmosphere is warming appears counterintuitive, and additional analyses should be conducted before reaching definitive conclusions as to the temporal trend obtained in the watersheds, as it may be related to climate model structure. More specifically, one cause may be related to the trends in extreme precipitation and/or maximization ratios produced by, or derived from, the CRCM as the climate shifts. Fig. 9 shows the summer-fall extreme precipitation events that led to the PMP values. As expected, there is a general increasing trend for extreme events, which was also found by others (e.g. Mailhot et al., 2007). This means that the maximization ratio of Eq. (1) is decreasing in the future, at least for those two climate models in the Moisie watershed.

Whether such trends are expected remains to be confirmed. However, as the atmospheric moisture holding capacity increases with increasing air temperature, the trend for the maximization ratio can theoretically decrease or increase. Indeed, the maximization ratio is composed of two variables: maximum precipitable water and actual precipitable water. Maximum precipitable water (the numerator in the maximization ratio) is likely to increase in the future as air temperature rises (Clark, 1987; Kunkel et al., 2013). It is limited by an upper bound

for a given temperature, corresponding to atmospheric saturation. For example, this upper bound for the Gulf Coast in the USA was found to be 75 mm in the past 50 years for the summer season (Kunkel et al., 2013). An increase of the actual precipitable water is also a possibility in the future because the atmospheric capacity to hold water vapor increases with warmer temperatures. However, depending on the magnitude of this increase relative to a corresponding increase of the maximum precipitable water, the net effect could be either a rise or a reduction of the maximization ratio. It is therefore the combination of both trends – extreme precipitation events and maximization ratios – in Eq. (1) that can result in either an increasing or a decreasing trend in future PMP. Klein et al. (2016) analyzed climate change influence on the maximization ratio for two watersheds in the province of Quebec. They found that the number of CRCM tiles with maximization ratio exceeding 2.5 (set as an upper limit) decreases in the future. This can be interpreted as an overall reduction of the maximization ratio.

This also raises a question about the validity of Eq. (1) for estimating PMP. For example, convective activities in North America are expected to increase in future climate scenarios (Paquin et al., 2014). Therefore, the occurrence of convective rainfall of increased severity is more likely. Averaged CAPE for all simulations shows that CAPE increased by 68, 51, and 52% in the future for the Chaudière, Moisie and Great Whale watersheds, respectively. Yet, severe convective storms can be sustained with moderate precipitable water values, as they are fed by atmospheric convective activity during rainfall. This process is not taken into account by the moisture maximization PMP estimation method as described by Eq. (1).

The validity of Eq. (1) has been challenged with the conclusion that the linear relationship in this equation does not hold in some cases (Abbs, 1999). To resolve this issue, attempts were made to estimate PMP using numerical weather models (Ohara et al., 2011). Although not constrained by assumptions such as in Eq. (1), output of these models is not necessarily PMP, but rather Maximum Precipitation (MP), as its calculation is deterministic and based on boundary conditions fed to the model, representing extreme atmospheric conditions leading to severe storms.

Results from this research show that there are multiple factors that influence the PMF values in watersheds dominated by snow processes. The Great Whale watershed, which is the largest in terms of surface area, has a smaller spring PMF value compared to the Moisie watershed. This is because the spring PMP and  $S_{100}$  in the Moisie watershed are larger by up to 24% and 31%, respectively, and the melt is occurring faster since the watershed is located at a lower latitude than Great Whale. Therefore, the surface area alone is not necessarily the major contributor to the PMF value. A similar conclusion was reported for Asian watersheds (Bao Quang and Laituri, 2013).

Finally, one may argue that 48- or even 72-h PMP events should have been selected to estimate PMF in this study, as larger watersheds usually demand longer PMP duration. Indeed, in designing hydraulic structures such as dam spillways, the optimal duration of PMP should be the one which produces the largest PMF; which is linked to watershed area. However, the goal of this paper is not producing PMF values to be used for design purposes; but rather to investigate how PMF is expected to change as the climate shifts. Therefore we believe that the choice of a 24-h PMP event to compute its corresponding PMF event is justified in this context. Note that in a research by Beauchamp et al. (2013), who used 24- to 72-h summer PMP events to calculate corresponding PMF on the Manicouagan River watershed in Québec, which is of similar size of the larger watershed used in our study, their authors actually obtained a smaller 72-h PMF as compared to the 48-h event, as the larger magnitude of the storm was distributed over a longer duration, reinforcing the hypothesis that an optimal PMP duration will produce the largest PMF value of a given watershed.

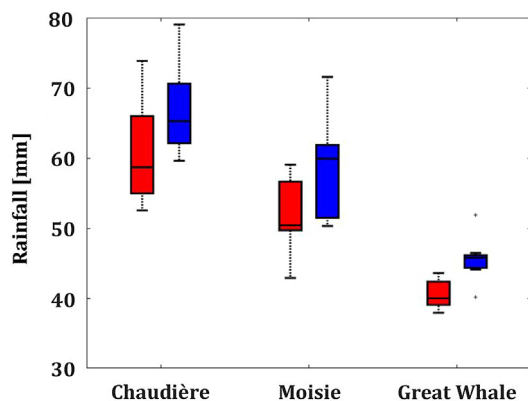


Fig. 9. Extreme events that produce PMP values for three watersheds. Red and blue colors refer to reference and future time horizon, respectively. (For interpretation of the references to colour in this figure legend, the reader is referred to the web version of this article.)

## 6. Conclusion

In this paper, the influence of climate change on PMP and PMF for three northern watersheds with different climate and physiographic characteristics was studied. The watersheds are located in southern, central and northern regions of the province of Québec, Canada. To simulate climate change conditions, projected climate data of seven simulations using the CRCM model with different GCM forcings, GHG emission scenarios and initial conditions were used, providing climate data that include daily precipitation, temperature, specific humidity, CAPE and SWE with a spatial resolution of 45 km. PMP for two time horizons, 1961–1990 and 2041–2070, were estimated through a deterministic approach based on the WMO and adapted to climate change impact studies by (Rouhani and Leconte, 2016).

The PMP values were estimated for two different seasons, summer-fall and spring, which produced two PMF values. Based on the results, the spring PMF was found to be larger than the summer-fall PMF for all watersheds and all time horizons. Therefore, the all-season PMF should be estimated from spring scenarios. The spring PMF in the Chaudière watershed located in southern Québec would increase by 3% in the future time horizon, while in the Moisie and Great Whale watersheds (respectively located in central and northern Québec) an 8 and 11% increase were obtained for these two respective watersheds (scenario 1). The magnitude of the trends is closely tied to the interactions between the PMP,  $S_{100}$  and temperature time series used to melt the snowpack. The largest PMF is obtained for the Moisie watershed although its surface area is much smaller than that of the Great Whale watershed. Finally, these results were obtained using seven climate projections from the CRCM. While PMP appears to be underestimated, along with an underestimation of the PMF, the temporal trends are a reasonable indicator of future changes in spring PMF resulting from climate change.

Finally, this study did not consider all sources of uncertainty that may affect the results. We considered uncertainties due to climate variability, initial conditions and GHG scenarios. However, yet there are other sources of uncertainties. For example, only one regional climate model and one hydrological model were used. Including more models would help to quantify uncertainties due to downscaling (many RCMs) and hydrological model structure/parameters (many hydrological models). Chen et al. (2011) have demonstrated that downscaling techniques may introduce significant uncertainty in estimating spring peak flow, and by extension, PMF. Also, the SWAT hydrological model uses a simplified snow melt routine based on the temperature index method and also calculates flow at a daily time step. Having other models with a diversity of snowmelt equations and sub-daily time steps would allow investigating their effect on spring peak flows, as in Chen et al. (2011), and therefore assessing model uncertainty on spring PMF.

## Acknowledgments

We wish to thank the Natural Sciences and Engineering Research Council of Canada for funding this research. The CRCM data was generated and supplied by Ouranos. For more information, please visit [www.ouranos.ca](http://www.ouranos.ca).

## References

- Abbs, D.J., 1999. A numerical modeling study to investigate the assumptions used in the calculation of probable maximum precipitation. *Water Resour. Res.* 35 (3), 785–796.
- AghaKouchak, A., Easterling, D., Hsu, K., Schubert, S., Sorooshian, S., 2012. *Extremes in a Changing Climate: Detection, Analysis and Uncertainty*. Springer Science & Business Media.
- Arnell, N.W., 1998. Climate change and water resources in Britain. *Clim. Change* 39 (1), 83–110.
- Arnold, J. et al., 2012. *Soil and Water Assessment Tool Input/Output Documentation 2012*. Texas Water Resources Institute Technical Report(439).
- Bao Quang, T., Laituri, M., 2013. The effects of watershed characteristics on storm runoff relationships in Vietnam. *J. Environ. Sci. Water Resour.* 2 (2), 13.
- Bates, B., Kundzewicz, Z.W., Wu, S., Palutikof, J., 2008. *climate change and Water: technical Paper vi*. Intergovernmental Panel on Climate Change (IPCC).
- Beauchamp, J., Leconte, R., Trudel, M., Brissette, F., 2013. Estimation of the summer-fall PMP and PMF of a northern watershed under a changed climate. *Water Resour. Res.* 49 (6), 3852–3862.
- Bernstein, L. et al., 2007. *Climate Change: Synthesis Report: An Assessment of the Intergovernmental Panel on Climate Change*. IPCC Plenary XXVII (Valencia, Spain 12–17 November 2007).
- Caya, D., Laprise, R., 1999. A semi-implicit semi-Lagrangian regional climate model: the Canadian RCM. *Month. Weath. Rev.* 127 (3), 341–362.
- CEHQ, 2015. *Atlas hydroclimatique du Québec méridional – Impact des changements climatiques sur les régimes de crue, d'étiage et d'hydraulicité à l'horizon 2050*, Centre d'expertise hydrique du Québec Ministère du Développement durable, de l'Environnement et de la Lutte contre les changements climatiques, Quebec.
- CEHQ, SNC-Lavalin, 2003. *Estimation des conditions hydrometeorologiques conduisant aux crues maximales probable (CMP) au Quebec*. Pluies, SNC-Lavalin, Division Energie.
- CEHQ, SNC-Lavalin, 2004. *Estimation des conditions hydrometeorologiques conduisant aux crues maximales probable (CMP) au Quebec*. Rapport Final, SNC-Lavalin, Division Energie.
- Chen, J., Brissette, F.P., Leconte, R., 2011. Uncertainty of downscaling method in quantifying the impact of climate change on hydrology. *J. Hydrol.* 401 (3), 190–202.
- Chernet, H.H., Alfredeen, K., Midttømme, G.H., 2013. Safety of hydropower dams in a changing climate. *J. Hydrol. Eng.* 19 (3), 569–582.
- Chow, K., Jones, S., 1994a. Probable maximum flood in boreal regions. Prepared par Atria Engineering Hydraulics pour l'Association Canadienne d'Electricite. ACE (9111).
- Chow, K.C.A., Jones, S.B., 1994b. Probable Maximum Floods in Boreal Regions. Prepared by Atria Engineering Hydraulics Inc for Canadian Electrical Association. Canadian Electrical Association.
- Clark, R.A., 1987. Hydrologic design criteria and climate variability. *IAHS Publ.* 168, 640.
- Clavet-Gaumont, J., et al., 2017. Probable maximum flood in a changing climate: an overview for Canadian basins. *J. Hydrol. Reg. Stud.* 13, 11–25. <http://dx.doi.org/10.1016/j.ejrh.2017.07.003>.
- Comité de Bassin de la Rivière Chaudière, 2015. *Territoire du COBARIC*, Sainte-Marie (Québec).
- Condon, L., Gangopadhyay, S., Pruitt, T., 2015. Climate change and non-stationary flood risk for the upper Truckee River basin. *Hydrol. Earth Syst. Sci.* 19 (1), 159–175.
- de Elia, R., Côté, H., 2010. Climate and climate change sensitivity to model configuration in the Canadian RCM over North America. *Meteorol. Z.* 19 (4), 325–339.
- Debs, I., Sparks, D., Rousselle, J., Birikundavyi, S., 1999. Évaluation des méthodes utilisées pour l'estimation de la crue maximale probable en régions nordiques. *Can. J. Civ. Eng.* 26 (3), 355–367.
- Desrochers, G.E. et al., 2008. Impacts des changements climatiques sur les apports en eau des bassins versants du Québec, 3e symposium scientifique Ouranos les 19 et 20 novembre à Montréal. Ouranos Montréal.
- DeWalle, D.R., Rango, A., 2008. *Principles of Snow Hydrology*. Cambridge University Press.
- Duan, Q., Sorooshian, S., Gupta, V., 1992. Effective and efficient global optimization for conceptual rainfall-runoff models. *Water Resour. Res.* 28 (4), 1015–1031.
- Durman, C., Gregory, J.M., Hassell, D.C., Jones, R., Murphy, J., 2001. A comparison of extreme European daily precipitation simulated by a global and a regional climate model for present and future climates. *Q. J. R. Meteorol. Soc.* 127 (573), 1005–1015.
- Ely, P.B., Peters, J.C., 1984. Probable maximum flood estimation-eastern United States1. *JAWRA* 20 (3), 391–396.
- Environment and Climate Change Canada, 2013. *Canada's Top Ten Weather Stories for 2011*.
- Environment Canada, 2015. *Canadian climate normals 1981–2010*. Environment Canada.
- Foulon, É., Rousseau, A.N., Gagnon, P., 2017. Development of a methodology to assess future trends in low flows at the watershed scale using solely climate data. *J. Hydrol.*
- Frei, C., Schär, C., Lüthi, D., Davies, H.C., 1998. Heavy precipitation processes in a warmer climate. *Geophys. Res. Lett.* 25 (9), 1431–1434.
- Gao, S., Li, X., 2008. *Cloud-Resolving Modeling of Convective Processes*. Springer Science & Business Media.
- Gouvernement du Québec, 2015a. *Développement durable, Environnement et Lutte contre les changements climatiques*. Bassin versant de la rivière Moisie.
- Gouvernement du Québec, 2015b. *Loi sur la sécurité des barrages*. Publications du Québec, Québec, Canada.
- Goyette, S., Beniston, M., Caya, D., Laprise, R., Junjo, P., 2001. Numerical investigation of an extreme storm with the Canadian Regional Climate Model: the case study of windstorm VIVIAN, Switzerland, February 27, 1990. *Clim. Dyn.* 18 (1–2), 145–168.
- Groisman, P.Y., et al., 2005. Trends in intense precipitation in the climate record. *J. Clim.* 18 (9), 1326–1350.
- Groisman, P.Y., Knight, R.W., Zolina, O.G., Pielke, R., 2013. Recent trends in regional and global intense precipitation patterns. *Clim. Vulnerab.* 5, 25–55.
- Haguma, D., 2013. *Gestion des ressources hydriques adaptée aux changements climatiques pour la production optimale d'hydroélectricité*. Étude de cas: bassin versant de la rivière Manicouagan. Université de Sherbrooke, Sherbrooke.
- Hempel, S., Frieler, K., Warszawski, L., Schewe, J., Piontek, F., 2013. A trend-preserving bias correction—the ISI-MIP approach. *Earth Syst. Dyn.* 4 (2), 219–236.
- Hutchinson, M.F., et al., 2009. Development and testing of Canada-wide interpolated spatial models of daily minimum-maximum temperature and precipitation for 1961–2003. *J. Appl. Meteorol. Climatol.* 48 (4), 725–741.
- Hydro-Québec, SNC-Shawinigan, 1992. *Recommendation of the expert committee on the determination of a realistic scenario for probable maximum flood on the St. Maurice river basin*.
- International Institute for Applied Systems Analysis, 2015. *Harmonized World Soil*

- Database.
- International Joint Commission, 2015. A real-time flood forecasting and flood inundation mapping system for the Lake Champlain-Richelieu River watershed, International Lake Champlain – Richelieu River Technical Working Group.
- IPCC, 2012. Managing the Risks of Extreme Events and Disasters to Advance Climate Change Adaptation: Special Report of the Intergovernmental Panel on Climate Change. Cambridge University Press.
- Jakob, D., Smalley, R., Meighen, J., Taylor, B., Xuereb, K., 2008. Climate change and probable maximum precipitation.
- Karl, T.R., Knight, R.W., Easterling, D.R., Quayle, R.G., 1996. Indices of climate change for the United States. *Bull. Am. Meteorol. Soc.* 77 (2), 279–292.
- Karl, T.R., et al., 2008. Weather and climate extremes in a changing climate: Regions of focus. US Climate Change Science Program, North America, Hawaii, Caribbean, and US Pacific Islands.
- Klein, I.M., Rousseau, A.N., Frigon, A., Freudiger, D., Gagnon, P., 2016. Evaluation of probable maximum snow accumulation: development of a methodology for climate change studies. *J. Hydrol.* 537, 74–85.
- Koutsoyiannis, D., 1999. A probabilistic view of Hershfield's method for estimating probable maximum precipitation. *Water Resour. Res.* 35 (4), 1313–1322.
- Kunkel, K.E., et al., 2013. Probable maximum precipitation and climate change. *Geophys. Res. Lett.* 40 (7), 1402–1408.
- Lagos-Zúñiga, M.A., Vargas, M.X., 2014. PMP and PMF estimations in sparsely-gauged Andean basins and climate change projections. *Hydrol. Sci. J.* 59 (11), 2027–2042.
- Langousis, A., Mamalakis, A., Deidda, R., Marrocu, M., 2016. Assessing the relative effectiveness of statistical downscaling and distribution mapping in reproducing rainfall statistics based on climate model results. *Water Resour. Res.* 52 (1), 471–494.
- Lapointe, M., Secretan, Y., Driscoll, S., Bergeron, N., Leclerc, M., 1998. Response of the Ha! Ha! River to the flood of July 1996 in the Saguenay region of Quebec: large-scale avulsion in a glaciated valley. *Water Resour. Res.* 34 (9), 2383–2392.
- Mailhot, A., Beauregard, I., Talbot, G., Caya, D., Biner, S., 2012. Future changes in intense precipitation over Canada assessed from multi-model NARCCAP ensemble simulations. *Int. J. Climatol.* 32 (8), 1151–1163.
- Mailhot, A., Duchesne, S., Caya, D., Talbot, G., 2007. Assessment of future change in intensity–duration–frequency (IDF) curves for Southern Quebec using the Canadian Regional Climate Model (CRCM). *J. Hydrol.* 347 (1), 197–210.
- Menzel, L., Bürger, G., 2002. Climate change scenarios and runoff response in the Mulde catchment (Southern Elbe, Germany). *J. Hydrol.* 267 (1), 53–64.
- Milbrandt, J., Yau, M., 2001. A mesoscale modeling study of the 1996 Saguenay flood. *Month. Weath. Rev.* 129 (6), 1419–1440.
- Milly, P.C.D., Wetherald, R.T., Dunne, K., Delworth, T.L., 2002. Increasing risk of great floods in a changing climate. *Nature* 415 (6871), 514–517.
- Minville, M., Brisette, F., Leconte, R., 2008. Uncertainty of the impact of climate change on the hydrology of a nordic watershed. *J. Hydrol.* 358 (1–2), 70–83. <http://dx.doi.org/10.1016/j.jhydrol.2008.05.033>.
- Mirhosseini, G., Srivastava, P., Stefanova, L., 2013. The impact of climate change on rainfall Intensity–Duration–Frequency (IDF) curves in Alabama. *Reg. Environ. Change* 13 (1), 25–33.
- Mishra, V., Ganguly, A.R., Nijssen, B., Lettenmaier, D.P., 2015. Changes in observed climate extremes in global urban areas. *Environ. Res. Lett.* 10 (2), 024005.
- Morgan, M.G., Henrion, M., Small, M., 1992. Uncertainty: A Guide to Dealing with Uncertainty in Quantitative Risk and Policy Analysis. Cambridge University Press.
- Music, B., Caya, D., 2007. Evaluation of the hydrological cycle over the Mississippi River basin as simulated by the Canadian Regional Climate Model (CRCM). *J. Hydrometeorol.* 8 (5), 969–988.
- Nakicenovic, N. et al., 2000. Emissions scenarios. IPCC.
- Nash, J., Sutcliffe, J.V., 1970. River flow forecasting through conceptual models part I—a discussion of principles. *J. Hydrol.* 10 (3), 282–290.
- Natural Resources Canada, 2015. Canadian Digital Elevation Model (CDEM).
- Neitsch, S., Arnold, J., Kiniry, J.e.a., Srinivasan, R., Williams, J., 2002. Soil and water assessment tool user's manual version 2000. GSWRL report, 202(02-06).
- Ohara, N., et al., 2011. Physically based estimation of maximum precipitation over American River watershed, California. *J. Hydrol. Eng.* 16 (4), 351–361.
- Oreskes, N., Shrader-Frechette, K., Belitz, K., 1994. Verification, validation, and confirmation of numerical models in the earth sciences. *Science* 263 (5147), 641–646.
- Paquet, E., Garavaglia, F., Garçon, R., Gailhard, J., 2013. The SCHADEX method: a semi-continuous rainfall–runoff simulation for extreme flood estimation. *J. Hydrol.* 495, 23–37.
- Paquin, D., 2010. Évaluation du MRCC4 en passé récent (1961–1999), Internal report-Climate simulation group, Ouranos.
- Paquin, D., de Elia, R., Frigon, A., 2014. Change in North American atmospheric conditions associated with deep convection and severe weather using CRCM4 climate projections. *Atmos. Ocean* 52 (3), 175–190.
- Petersen, A.C., 2000. Philosophy of climate science. *Bull. Am. Meteorol. Soc.* 81 (2), 265.
- Prasad, R., Hibler, L.F., Coleman, A.M., Ward, D.L., 2011. Design-basis flood estimation for site characterization at nuclear power plants in the United States of America. Pacific Northwest National Laboratory (PNNL), Richland, WA (US).
- Qian, B., Zhang, X., Chen, K., Feng, Y., O'Brien, T., 2010. Observed long-term trends for agroclimatic conditions in Canada. *J. Appl. Meteorol. Climatol.* 49 (4), 604–618. <http://dx.doi.org/10.1175/2009jamc2275.1>.
- Rastogi, D., et al., 2017. Effects of climate change on probable maximum precipitation: a sensitivity study over the Alabama-Coosa-Tallapoosa River Basin. *J. Geophys. Res. Atmosph.* 122 (9), 4808–4828. <http://dx.doi.org/10.1002/2016jd026001>.
- Roekner, E. et al., 2003. The atmospheric general circulation model ECHAM 5. PART I: Model description.
- Rouhani, H., 2016. Les effets du changement climatique sur la pluie maximale probable et la crue maximale probable au Québec. Université de Sherbrooke, Sherbrooke pp. 151.
- Rouhani, H., Leconte, R., 2016. A novel method to estimate the maximization ratio of the Probable Maximum Precipitation (PMP) using regional climate model output. *Water Resour. Res.* 52 (9), 7347–7365.
- Rousseau, A., Gagnon, P., Savary, S., Freudiger, D., Klein, I., 2012. Intégration de l'impact des changements climatiques (CC) dans la détermination des crues maximales probables (CMP) afin d'appuyer les usagers dans l'évaluation de la sécurité des barrages, Final report No. R-1385 presented to Ouranos Consortium, Québec city, PQ, Canada.
- Rousseau, A.N., et al., 2014. Development of a methodology to evaluate probable maximum precipitation (PMP) under changing climate conditions: application to southern Quebec, Canada. *J. Hydrol.* 519, 3094–3109.
- Roy, L., Leconte, R., Brisette, F.P., Marche, C., 2001. The impact of climate change on seasonal floods of a southern Quebec River Basin. *Hydrol. Process.* 15 (16), 3167–3179.
- Salas-Méila, D., et al., 2005. Description and validation of the CNRM-CM3 global coupled model. *Clim. Dynam.* 103, 1–36.
- Schmidli, J., Frei, C., Vidale, P.L., 2006. Downscaling from GCM precipitation: a benchmark for dynamical and statistical downscaling methods. *Int. J. Climatol.* 26 (5), 679–689.
- Scholze, M., Knorr, W., Arnell, N.W., Prentice, I.C., 2006. A climate-change risk analysis for world ecosystems. *Proc. Natl. Acad. Sci.* 103 (35), 13116–13120.
- Schreiner, L.C., Riedel, J.T., 1978. Probable maximum precipitation estimates, United States east of the 105th meridian. Department of Commerce National Oceanic and Atmospheric Administration.
- Solomon, S., et al., 2007. The Physical Science Basis, Contribution of Working Group I to the Fourth Assessment Report of the Intergovernmental Panel on Climate Change. Cambridge University Press, Cambridge, United Kingdom and New York, NY, USA.
- Stainforth, D.A., Allen, M.R., Tredger, E.R., Smith, L.A., 2007. Confidence, uncertainty and decision-support relevance in climate predictions. *Philosoph. Trans. R. Soc. Lon. A: Mathem. Phys. Eng. Sci.* 365 (1857), 2145–2161.
- Stewart, I.T., Cayan, D.R., Dettinger, M.D., 2005. Changes toward earlier streamflow timing across western North America. *J. Clim.* 18 (8), 1136–1155.
- Stratz, S.A., Hossain, F., 2014. Probable maximum precipitation in a changing climate: Implications for dam design. *J. Hydrol. Eng.* 19 (12), 06014006.
- Tofiq, F., Güven, A., 2015. Potential changes in inflow design flood under future climate projections for Darbandikhan Dam. *J. Hydrol.* 528, 45–51.
- Vescovi, L., Baril, P., Desjarlais, C., Musy, A., Roy, R., 2009. Water and climate change in Quebec. Scientific Paper published in the Side publication series of the World Water Assessment Programme of UNESCO, 12pp. Pacher, G., Minville, M., Frigon, A., Roy, R., Slivitzky, M.(2009), Climate change and water resources: an approach to adaptive Management, The Role of Hydrology in Water Resources Management. IAHS Publ, 327: 97-103.
- WMO, 1973. Manual on Estimation of Probable Maximum Precipitation (PMP). World Meteorological Organization, Geneva.
- WMO, 1986. Manual on Estimation of Probable Maximum Precipitation (PMP). World Meteorological Organization, Geneva.
- WMO, 2009. Manual on Estimation of Probable Maximum Precipitation (PMP). World Meteorological Organization, Geneva.
- Yagouti, A., Boulet, G., Vincent, L., Vescovi, L., Mekis, E., 2008. Observed changes in daily temperature and precipitation indices for southern Québec, 1960–2005. *Atmos. Ocean* 46 (2), 243–256.